THE ASTROPHYSICAL JOURNAL, 551:L45–L48, 2001 April 10

THE EVOLUTION OF THE LUMINOSITY FUNCTION IN DEEP FIELDS: A COMPARISON WITH COLD DARK MATTER MODELS

F. POLI,[1] N. MENCI,[1] E. GIALLONGO,[1] A. FONTANA,[1] S. CRISTIANI,[2] AND S. D'ODORICO[3]
Received 2001 January 3; accepted 2001 March 1; published 2001 April 4

ABSTRACT

The galaxy luminosity function (LF) has been estimated in the rest-frame B luminosity at $0 < z < 1.25$ and at 1700 Å for $2.5 < z < 4.5$ from deep multicolor surveys in the Hubble Deep Field–North, the Hubble Deep Field–South, and the New Technology Telescope Deep Field. The results have been compared with a recent version of galaxy formation models in the framework of hierarchical clustering in a flat cold dark matter universe with cosmological constant. The results show a general agreement for $z \lesssim 1$, although the model LF has a steeper average slope at the faint end; at $z \sim 3$ such a feature results in an overprediction of the number of faint ($I_{AB} \sim 27$) galaxies, while the agreement at the bright end becomes critically sensitive to the details of dust absorption at such redshifts. The discrepancies at the faint end show that a refined treatment of the physical processes involving smaller galaxies is to be pursued in the models, in terms of aggregation processes and/or stellar feedback heavily affecting the luminosity of the low-luminosity objects. The implications of our results on the evolution of the cosmological star formation rate are discussed.

Subject headings: galaxies: evolution — galaxies: formation — galaxies: fundamental parameters

1. INTRODUCTION

The evolution of the luminosity function (LF) is a fundamental probe for cosmological theories of galaxy formation. Indeed, the red and blue/UV luminosities are related to the galaxy stellar mass and star formation rate, respectively. Thus, the evolution of the LF reflects the differential contribution of different galaxy types to the cosmic history of mass growth and of star formation, which are the main outcomes of hierarchical models for galaxy formation.

Adopting a Schechter fit to the LF, recent estimates (Zucca et al. 1997; Marzke & da Costa 1997; Folkes et al. 1999) point toward a relatively steep power law at the faint end (with a power index $\simeq$1.2), although an excess of dwarf blue galaxies relative to the Schechter fit is found at the faint end.

In the intermediate-redshift range (up to $z \sim 1$), first steps toward the evaluation of the LF evolution were undertaken by the Canada-France Redshift Survey (CFRS; Lilly et al. 1995) and by the Autofib Redshift Survey (Ellis et al. 1996; Heyl et al. 1997). These surveys have shown some increase in the number density of the fainter population together with some increase in the luminosity of the brighter blue fraction. These two effects are responsible for the strong increase with z of the average cosmic UV luminosity density (by a factor of 5–10) in the redshift interval $0 < z < 1$.

Deep multicolor surveys of galaxies represent an effective way to explore the galaxy distribution in the redshift interval $1 < z < 5$. Successful spectroscopic confirmation was obtained for the brightest fraction by Steidel et al. (1996, 1999). For the bulk of the population, reliable photometric redshifts are currently used (e.g., Connolly et al. 1997; Giallongo et al. 1998; Fernández-Soto, Lanzetta, & Yahil 1999; Fontana et al. 2000).

The average UV luminosity density resulting from these studies shows a flat distribution at $z > 1$ that extends up to $z \sim 4.5$. Such a result represents a strong constraint to hierarchical galaxy formation theories that predict a significant contribution by a large population of small objects. In a previous paper, we showed that when the effects of the sample magnitude limits are included in the models, a steady decline in the predicted UV luminosity density appears in contrast with the observed behavior (Fontana et al. 1999).

Attempts to clarify the contribution of different (in mass and star formation rate) galaxy populations to the global UV luminosity density requires an evaluation of the high-redshift LF down to the faintest accessible magnitudes. In this Letter, we present a first estimate of the intermediate/high-z LF using a composite deep multicolor sample of about 1200 galaxies with reliable photometric redshifts down to $I_{AB} = 27.5$. The depth of this data sample, together with its relatively large area, allows a direct comparison of the observed LF shape and evolution with theoretical predictions. Such comparison is performed using a semianalytic implementation of recent hierarchical models of galaxy formation.

2. THE DATA SAMPLE

The analyzed data set covers a wavelength range from the UV to the K bands, and observations were taken from ground-based telescopes and from the *Hubble Space Telescope* as well. The first field, known as the New Technology Telescope Deep Field (NTTDF), consists of an area of 4.84 arcmin^2, where optical and near-IR *UBVRIJK* observations have been taken at the ESO NTT with various instrumentation (SUSI, SUSI-2, SOFI). Further details about the multicolor catalog can be found in Arnouts et al. (1999) and in Fontana et al. (2000).

We have also used the Hubble Deep Field (HDF) North and South catalogs provided by Fernández-Soto et al. (1999), with an overall area of 3.92 and 4.22 arcmin^2, respectively. After appropriate selections to remove contamination by stars and low signal-to-noise ratio (S/N) regions, we applied our photometric redshift code to the data down to $I_{AB} = 27.5$. A detailed description of this procedure, along with photometric z catalogs, can be found in Fontana et al. (2000).

In addition, in the present evaluation of the LF, we have also considered one of the main systematic errors affecting the estimates of the galaxy total absolute magnitudes at various red-

[1] Osservatorio Astronomico di Roma, via dell'Osservatorio, I-00040 Monteporzio, Italy.
[2] ST European Coordinating Facility, Karl-Schwarzschild-Strasse 2, D-85748 Garching, Germany.
[3] European Southern Observatory, Karl-Schwarzschild-Strasse 2, D-85748 Garching, Germany.

shifts, which is the surface brightness cosmological dimming effect. To correct for this effect, one has to recover the total galaxy emitted flux. To estimate the systematic losses associated with any recovering procedure, we performed simulations of synthetic galaxies (having exponential intensity profiles with an ellipticity of 0.5) with different apparent magnitudes, as seen with the appropriate S/N in the HDF images. Then we compared the total input flux with the one obtained by extrapolating the intensity profiles as computed in the SExtractor package (Bertin & Arnouts 1996). The simulations show that the difference ΔI between the input and the measured apparent magnitudes increases from 0.1 to 0.25 when the input magnitude increases from $I \sim 25$ to $I \simeq 27.2$. For these reasons, although the catalogs in the HDFs go deeper, we will confine the analysis of the LF at magnitudes $I \leq 27.2$ in the HDFs (and 25.7 in the NTTDF), where errors in the estimate of the total magnitudes are small and do not affect our main results on the shape of the LF.

3. ESTIMATING THE LUMINOSITY FUNCTION

Several methods are available in the literature (see Efstathiou, Ellis, & Peterson 1988 for a discussion); here we choose to adopt the classical $1/V_{\max}$ estimator (Schmidt 1968) jointly with the Sandage, Tammann, & Yahil (1979) maximum likelihood fit for a Schechter function. In the $1/V_{\max}$ method, for any given redshift bin (z_1, z_2) an effective maximum volume is assigned to each object. This volume is enclosed between z_1 and $z_{\rm up}$, the latter being defined as the minimum between z_2 and the maximum redshift at which the object could have been observed given the magnitude limit of the sample.

Combining data from separate fields with different magnitude limits, we then compute the galaxy number density $\phi(M_B, z)$ in every $(\Delta z, \Delta M_B)$ bin as follows:

$$\phi(M_B, z) = \frac{1}{\Delta M_B} \sum_{i=1}^{N} \left[\sum_j \omega(j) \int_{z_1}^{z_{\rm up}(i,j)} \frac{dV}{dz} dz \right]^{-1}, \quad (1)$$

where $\omega(j)$ is the area in units of steradians corresponding to the field j and N is the total number of objects in the chosen bin. The number of fields involved in the sum over index j is restricted to the ones with a faint enough magnitude limit for the ith object to be detected. In this way each galaxy has a different $z_{\rm up}(j)$ in every field, and the overall volume available for this object is obtained summing the corresponding $V_{\max}(j)$.

On the other hand, the Sandage, Tammann, & Yahil (1979) technique, once assumed a Schechter behavior for the LF, is an endeavor to maximize the likelihood of representing the observed set of galaxies with the best-fit parameters of the Schechter function. Assuming that, in an appropriately thin bin of redshift, the number of sources with redshift between z and $z + dz$, and with absolute magnitude between M_B and $M_B + dM_B$, can be factorized as $\phi(M_B, z)dz\, dM_B = \rho(z)\psi(M_B)dz\, dM_B$, where $\rho(z)$ is the density of galaxies at redshift z, that can be considered constant within the bin. The function $\psi(M_B)$ is taken to have a Schechter form, parametrized by the characteristic absolute magnitude M_B^*, by the logarithmic slope at the faint-end α and by the normalization ψ_*.

If we choose an appropriate redshift bin (z_1, z_2), it is possible to give an estimation of α and M_B^* considering the probability density $p_{i,j}$ to find a galaxy with redshift in the range $z_i, z_i + dz$ and absolute magnitude between M_i and $M_i + dM$ in the jth magnitude-limited field and maximizing the likelihood of observing the set of galaxies that comes from the surveys, which is simply given by the product of the single probabilities:

$$\prod_j \prod_{i=1}^{N_j} p_{i,j} = \prod_j \prod_{i=1}^{N_j} \frac{\rho(z_i)\psi(M_i)dz\, dM}{\omega(j) \int_{z_1}^{z_2} \rho(z)(dV/dz)dz \int_{-\infty}^{M_{\rm lim}^{i,j}(z)} \psi(M)dM}, \quad (2)$$

$\omega(j)$ being the field area in units of steradians and $M_{\rm lim}^{i,j}(z)$ the absolute magnitude value that the ith object, if detected with the magnitude limit $m_{\rm lim}^j$ in the jth survey, should have at that redshift. This value clearly depends on the details of the spectrum of each object. Here j runs over the number of fields where the ith galaxy can be detected, each one containing N_j objects.

The value of ϕ^* is then obtained by summing the density in the z, M space for every galaxy, taking account of all the fields where it could be detected (i.e., the fields with enough bright magnitude limit):

$$\phi^* = \sum_{i=1}^{N_j} \left[\sum_{j_{\rm detect}} \omega(j) \int_{z_1}^{z_2} \frac{dV}{dz} dz \int_{-\infty}^{M_{\rm lim}^{i,j}(z)} \psi(M)dM \right]^{-1}. \quad (3)$$

As for an appropriate selection in magnitude of the sample, it is important to bear in mind that once a rest-frame wavelength λ is chosen (e.g., the 4400 Å band), this corresponds to different observed wavelengths $\lambda(1 + z)$ when z runs inside the redshift bin (z_1, z_2). Since our aim is to choose appropriately a complete subsample selected in the rest frame, we ought to take into account the different redshifts of each galaxy, and the details of the spectra as well, to be sure that we are selecting objects in a coherent way. One major concern is fixing the bins in redshift in a suitable way for matching the observed bands once the wavelength displacement is taken into account. Subsequently, the right selection criterion can be achieved by comparing the photometric limit with the $\lambda(1 + z)$ magnitude value taken from the spectrum. This implies a limiting magnitude ≤ 27.2 at a wavelength of $4400(1 + z)$ Å for $z \leq 1.25$ and ≤ 27.2 at $1700(1 + z)$ Å for $z > 2.5$ in the HDFs.

4. THE COSMOLOGICAL EVOLUTION OF THE LF

The LF at the rest-frame B magnitude in the AB system, M_B, is shown in Figure 1 for three redshift bins (0.2–0.5, 0.5–0.75, 0.75–1.25). The left panels refer to a critical universe with $\Omega_M = 1$, $\Omega_\Lambda = 0$, and $H_0 = 50$ km s^{-1} Mpc^{-1}, while the right panels refer to a flat universe dominated by the cosmological constant $\Omega_M = 0.3$, $\Omega_\Lambda = 0.7$, and $H_0 = 70$ km s^{-1} Mpc^{-1}. The rest-frame B magnitude is computed from the best-fit theoretical spectral energy distribution used to derive the photometric redshift. The magnitude limit of the sample has been evaluated at the same rest-frame wavelength centered in the rest-frame B band, which roughly corresponds to the observed V, R, and I bands for the three redshift bins, respectively. In addition, we show in Figure 2 the 1700 Å rest-frame LF in the bins $2.5 < z < 3.5$ and $3.5 < z < 4.5$ for the same cosmologies.

The best-fit values of the Schechter parameters obtained from the maximum likelihood method are summarized in Table 1 together with the relevant sample parameters for both the considered cosmologies. In the highest redshift bin ($3.5 < z < 4.5$) the small number of objects prevented an accurate estimate of the Schechter parameters. The Schechter curves corresponding to the tabulated fitting parameters are shown in Figures 1

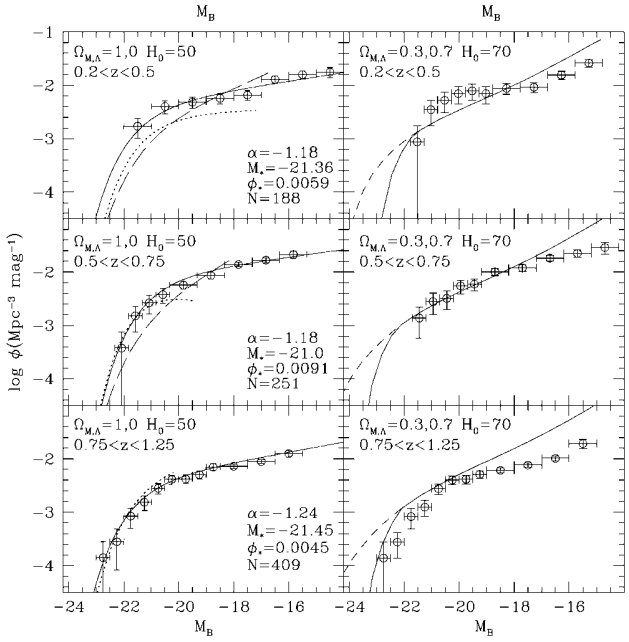

FIG. 1.—Rest-frame *B* LF of field galaxies in different redshift bins and for two cosmological models. *Left panels:* The continuous curves are the Schechter LFs resulting from the maximum likelihood fit to our composite galaxy sample. Dotted curves are the Schechter functions derived from the CFRS survey (Lilly et al. 1995), while the dashed curves are derived from the Autofib redshift survey (Heyl et al. 1997). *Right panels:* Continuous curves are the CDM model predictions discussed in the text, including dust absorption with a Small Magellanic Cloud extinction curve (different extinction curves used in Fig. 2 do not produce appreciable changes in the *B*-band LFs). Dashed curves are the CDM dust-free model predictions.

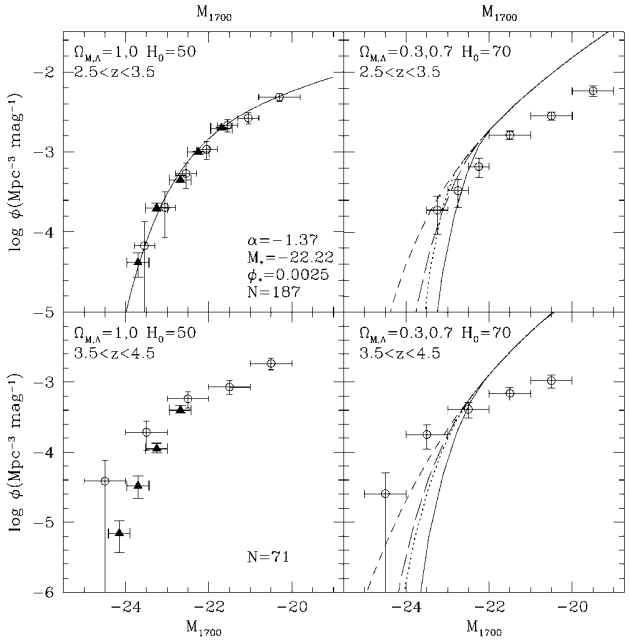

FIG. 2.—Rest-frame ultraviolet LF at $z \sim 3$ and $z \sim 4$. Filled symbols are derived from the spectroscopic survey by Steidel et al. (1999). *Left panels:* Continuous curve is derived from the Schechter maximum likelihood fit, as in Fig. 1. *Right panels:* Symbols as in the corresponding panel in Fig. 1, except for the dotted or long-dashed curves, which refer to the Milky Way and Calzetti extinction curves, respectively.

and 2 only for the case of the critical universe (*left panels*) for comparison with previous LFs computed in the same cosmology. In particular, the Schechter LFs from the CRFS and the Autofib survey are also shown for $z < 1.25$ as dotted and dashed curves, respectively. An overall agreement with the spectroscopic data is evident at bright magnitudes, supporting the reliability of our LF photometric estimation. The variance between spectroscopic surveys could be due to different *k*-corrections applied for the estimate of the rest-frame blue magnitudes from samples selected in different bands.

As discussed in Sawicki, Lin, & Yee (1997), the uncertainties in the photometric redshift estimates do not affect appreciably the behavior of the LF; suitable Monte Carlo simulations have shown that perturbations arising from redshift uncertainties result in effects smaller than 1 σ error bars in the $1/V_{\max}$ estimator and in small changes in the best-fit Schechter parameters. In our case, the good match with CFRS leaves little space for this kind of substantial change in the distribution.

It can be seen that from $z \sim 0.2$ up to $z \sim 1.25$, there is no evidence of a significant trend with redshift in the faint-end slope parameter α, which remains close to its local value $\alpha \simeq -1.2$ (Zucca et al. 1997). Also, the characteristic magnitude M_* shows a mild brightening with the look-back time.

At high redshifts a steepening effect is evident in the 1700 Å LF (Fig. 2, *left panel*), where the slope parameter reaches a value of -1.37, consistent within uncertainties with the $\alpha = -1.6$ found by Steidel et al. (1999) in an analogous redshift bin. We note, however, that in this high-redshift bin the slope is weakly constrained by the present depth of the galaxy sample.

5. A COMPARISON WITH HIERARCHICAL MODELS FOR GALAXY EVOLUTION

We compare our data with our rendition of the semianalytic models. The structure of such rendition is described in Poli et al. (1999). We updated our model to implement some of the most recent improvements inserted in the recent versions of semianalytic models, following the lines of Cole et al. (2000). In particular, we now adopt the Lacey & Cole (1993) dynamical friction timescale, the new star formation and feedback recipes, and the new modelization for hot gas distribution implemented by the above authors. This allows us to obtain a Tully-Fisher relation in reasonable agreement with observations together with a good fit to the local LF, the two observables that have been used to calibrate the free parameters governing the star formation and the feedback processes. In addition, we have included dust absorption, which is modeled as in Poli et al. (1999). We have checked that the predictions of our model

TABLE 1

PARAMETERS OF THE SCHECHTER FUNCTION FITS

z Range	α[a]	M_*[b]	ϕ_*	N
02–0.5	-1.18 ± 0.05	-21.36 ± 0.37	0.0059	188
	-1.19 ± 0.05	-21.03 ± 0.38	0.0086	...
0.5–0.75	-1.18 ± 0.06	-21.00 ± 0.29	0.0091	251
	-1.19 ± 0.06	-20.75 ± 0.30	0.01	...
0.75–1.25	-1.24 ± 0.06	-21.45 ± 0.24	0.0045	409
	-1.25 ± 0.05	-21.38 ± 0.25	0.0041	...
2.5–3.5	-1.37 ± 0.20	-22.22 ± 0.37	0.0025	187
	-1.37 ± 0.19	-22.34 ± 0.37	0.0023	...

[a] The second row for each z bin refers to the $\Omega_M = 0.3$, $\Omega_\Lambda = 0.7$ cosmology.

[b] M_* is M_B (AB) except in the $z = 2.5$–3.5 bin, where it is computed at 1700 Å, M_{1700}.

agree with those from Cole et al. (2000) for both the local observables and the global cosmic star formation history.

To compare with the data we focus on the flat ΛCDM (cold dark matter) cosmology. Such choice is favored by a significant amount of recent observational results, from the high fraction of the baryon–to–dark matter ratio in galaxy clusters (see, e.g., White & Fabian 1995) to the high-redshift supernovae (see Perlmutter et al. 1999). When inserted into galaxy formation models, the above set of parameters also yields a cosmic star formation history in reasonable agreement with observations (see Fontana et al. 1999), in contrast, e.g., with the standard CDM, with $\Omega_M = 1$ and $\Omega_\Lambda = 0$.

Figures 1 and 2 (*right panels*) show a comparison of the observed LFs derived from our composite sample and our CDM model. First we note a general agreement for $M_B < -20$ and $z \lesssim 1$. Both data and predictions show weak luminosity evolution resulting from a balance between a mild decrease with z of the number of massive objects and the increase of their star formation activity and hence of their blue luminosity. At the same time, the normalization of the LF rises by a factor of ~2.

At low luminosities the theoretical LF appears steeper than the observed one, with an excess at the faint end that becomes larger with increasing redshift. In addition, at $z > 2.5$ the model tends to slightly underestimate the magnitudes of bright galaxies when the model with larger dust extinction (~1 mag, in agreement with Pettini et al. 1998) is considered. Such results show that a refinement of the models is required, both in terms of dynamical processes (like merging of satellites in common halos; see Somerville, Primack, & Faber 2001) and in terms of stellar processes (like the feedback from supernovae, appreciably affecting the LF at the faint end). Indeed, the apparent agreement of the predicted versus observed UV luminosity density at $z > 2.5$ (Fontana et al. 1999) results from the balance in the LF between the excess of the predicted dwarfs and the deficit of predicted bright galaxies, as shown in the right panel of Figure 2.

This shows that the z-resolved LFs constitute a particularly powerful way of constraining the two most uncertain processes in the theoretical modeling, i.e., the dust absorption affecting the prediction of the number of bright galaxies and the supernova feedback affecting the slope of the predicted LF at the faint end.

The above considerations suggest that the comparison of the observed and predicted UV luminosity density at $z \geq 3$ is critical at the bright end. Indeed, the details of the dust extinction are important at the bright end of the steep LF function since the dust extinction affects not only the observed UV luminosities but also the number of galaxies that are detected within the magnitude limit. Some spectroscopic information for the brightest sources can better constrain the dust content at these high redshifts.

For such a reason, the comparison between the predicted and observed UV luminosity densities should be performed over wider areas of the sky, to reduce fluctuations in the number of bright sources, and using different limiting magnitudes, extended to the faintest limits, to explore the dust content as a function of the galaxy star formation rate and mass. This will allow us to sample the shape of the LF at the faint end, which is crucial to assess whether complementary physical processes have to be included in the current hierarchical models.

REFERENCES

Arnouts, S., D'Odorico, S., Cristiani, S., Zaggia, S., Fontana, A., & Giallongo, E. 1999, A&A, 341, 641
Bertin, E., & Arnouts, S. 1996, A&AS, 117, 393
Cole, S., Lacey, C., Baugh, C., & Frenk, C. 2000, MNRAS, 319, 168
Connolly, A. J., Szalay, A. S., Dickinson, M., SubbaRao, M. U., & Brunner, R. J. 1997, ApJ, 486, L11
Efstathiou, G., Ellis, R. S., & Peterson, B. A. 1988, MNRAS, 232, 431
Ellis, R. S., Colless, M. M., Broadhurst, T. J., Heyl, J. S., & Glazebrook, K. 1996, MNRAS, 280, 235
Fernández-Soto, A., Lanzetta, K. M., & Yahil, A. 1999, ApJ, 513, 34
Folkes, S., et al. 1999, MNRAS, 308, 459
Fontana, A., D'Odorico, S., Poli, F., Giallongo, E., Arnouts, A., Cristiani, S., Moorwood, A., & Saracco, P. 2000, AJ, 120, 2206
Fontana, A., Menci, N., D'Odorico, S., Giallongo, E., Poli, F., Cristiani, S., Moorwood, A., & Saracco, P. 1999, MNRAS, 310, L27
Giallongo, E., D'Odorico, S., Fontana, A., Cristiani, S., Egami, E., Hu, E., & McMahon, R. G. 1998, AJ, 115, 2169
Heyl, J., Colless, M., Ellis, R. S., & Broadhurst, T. 1997, MNRAS, 285, 613
Lacey, C., & Cole, S. 1993, MNRAS, 262, 627
Lilly, S., Tresse, L., Hammer, F., Crampton, D., & Le Fèvre, O. 1995, ApJ, 455, 108
Lin, H., Yee, H. K. C., Carlberg, R. C., Morris, S. L., Sawicki, M., Patton, D. R., Wirth, G., & Shepherd, C. W. 1999, ApJ, 518, 533
Marzke, L. O., & da Costa, L. N. 1997, AJ, 113, 185
Perlmutter, S., et al. 1999, ApJ, 517, 565
Pettini, M., Kellogg, M., Steidel, C. C., Dickinson, M., Adelberger, K. L., & Giavalisco, M. 1998, ApJ, 508, 539
Poli, F., Giallongo, E., Menci, N., D'Odorico, S., & Fontana, A. 1999, ApJ, 527, 662
Sandage, A., Tammann, G. A., & Yahil, A. 1979, ApJ, 232, 352
Sawicki, M. J., Lin, H., & Yee, H. K. C. 1997, AJ, 113, 1
Schmidt, M. 1968, ApJ, 151, 393
Somerville, R. S., Primack, J. R., & Faber, S. M. 2001, MNRAS, 320, 504
Steidel, C. C., Adelberger, K. L., Giavalisco, M., Dickinson, M., & Pettini, M. 1999, ApJ, 519, 1
Steidel, C. C., Giavalisco, M., Pettini, M., Dickinson, M., & Adelberger, K. L. 1996, ApJ, 462, L17
White, D. A., & Fabian, A. C. 1995, MNRAS, 273, 72
Zucca, E., et al. 1997, A&A, 326, 477